References

BITHER, T. A., DONOHUE, A. C. & YOUNG, H. S. (1971). *J. Solid State Chem.* **3**, 300–304.

BUCK, P. & CARPENTIER, C. D. (1973). *Acta Cryst.* B**29**, 1864–1868.

BUSING, W. R. (1966). Oak Ridge National Laboratory, Tennessee, USA.

CARPENTIER, C. D. (1974). Thesis, Univ. of Freiburg.

CARPENTIER, C. D., DIEHL, R. & NITSCHE, R. (1970). *Naturwissenschaften*, **57**, 393–394.

CROMER, D. T. & LIBERMAN, D. (1970). *J. Chem. Phys.* **53**, 1891–1898.

CROMER, D. T. & WABER, J. T. (1965). *Acta Cryst.* **18**, 104–109.

CRUICKSHANK, D. W. J. (1956). *Acta Cryst.* **9**, 747–753.

DIEHL, R. & CARPENTIER, C. D. (1976). *Acta Cryst.* B**32**, 1399–1404.

GAINES, R. V. (1957). *Am. Mineral.* **42**, 766–779.

GARIN, J. & PARTHÉ, E. (1972). *Acta Cryst.* B**28**, 3672–3674.

HAHN, H., FRANK, G., KLINGLER, W., STOERGER, A. D. & STOERGER, G. (1955). *Z. Anorg. Allg. Chem.* **279**, 241–270.

International Tables for X-ray Crystallography (1965). Vol. I, 2nd ed. Birmingham: Kynoch Press.

ISAACS, T. J., GOTTLIEB, M. & FEICHTNER, J. D. (1974). *Appl. Phys. Lett.* **24**, 107–109.

KATTY, A., SOLED, S. & WOLD, A. (1977). *Mater. Res. Bull.* **12**, 663–666.

KLINGEN, W., EULENBERGER, G. & HAHN, H. (1973). *Z. Anorg. Chem.* **401**, 97–112.

KLINGEN, W., OTT, R. & HAHN, H. (1973). *Z. Anorg. Allg. Chem.* **396**, 271–278.

LARSON, H. (1967). *Acta Cryst.* **23**, 664–666.

NITSCHE, R. & WILD, P. (1970). *Mater. Res. Bull.* **5**, 419–423.

SOKALOV, A. I. & NECHAEVA, V. V. (1969). *Izv. Akad. Nauk SSSR Neorg. Mater.* **5**, 989.

SOLED, S. & WOLD, A. (1976). *Mater. Res. Bull.* **11**, 657–662.

STEWART, J. M., KUNDELL, F. A. & BALDWIN, J. C. (1970). The XRAY 70 system. Computer Science Center, Univ. of Maryland, College Park, Maryland.

WEISS, A. & SCHAEFER, H. (1960). *Naturwissenschaften*, **47**, 495.

WEISS, A. & SCHAEFER, H. (1963). *Z. Naturforsch.* **18**, 81–82.

ZIMMERMANN, H., CARPENTIER, C. D. & NITSCHE, R. (1975). *Acta Cryst.* B**31**, 2003–2006.

Acta Cryst. (1978). B**34**, 1105–1111

The Crystal Structure of Triclinic WO_3

BY ROLAND DIEHL AND GERNOT BRANDT

Institut für Angewandte Festkörperphysik der Fraunhofer-Gesellschaft, Eckerstrasse 4, *D*-7800 *Freiburg im Breisgau, Federal Republic of Germany*

AND EKHARD SALJE

Mineralogisches Institut der Technischen Universität, Welfengarten 1, *D*-3000 *Hannover, Federal Republic of Germany*

(*Received* 26 *October* 1977; *accepted* 7 *November* 1977)

Between *ca* −40 and 17 °C tungsten trioxide, WO_3, has a pseudocubic triclinic crystal structure, space group $P\bar{1}$ (C_i^1), with $a = 7{\cdot}309$ (2), $b = 7{\cdot}522$ (2), $c = 7{\cdot}678$ (2) Å, $\alpha = 88{\cdot}81$ (2), $\beta = 90{\cdot}92$ (2), $\gamma = 90{\cdot}93$ (2)°, $V = 421{\cdot}93$ (9) Å^3, and $Z = 8$. Intensity data for 2452 independent X-ray reflections from a single-domain crystal were measured on an automatic four-circle single-crystal diffractometer. From analogies with the crystal structure of the monoclinic room-temperature modification of WO_3, the triclinic crystal structure was determined and refined to $R = 0{\cdot}050$. It is characterized by corner-sharing, and distorted and tilted WO_6 octahedra with a tilting component around each of the coordination axes. The W atoms are off-centre in the O octahedra and close to an O triangle, giving three short and three long W—O bonding distances.

Introduction

From 0 up to 1200 K stoichiometric tungsten trioxide, WO_3, is reported to undergo not less than eight phase transformations in the solid state (Levkowitz, Dowell & Shields, 1975; Rao & Rao, 1974). Crystallographic information has become available on the WO_3 phases which occur between 900 and −70 °C during cooling. Below 900 °C, WO_3 is tetragonal, space group $P4/nmm$ (D_{4h}^7) (Kehl, Hay & Wahl, 1952) and

transforms at about 740°C into an orthorhombic modification with space group *Pmnb* (D_{2h}^{16}) (Salje, 1977). Between *ca* 17 and 330°C WO_3 exhibits monoclinic symmetry, space group $P2_1/n$ (C_{2h}^5) (Tanisaki, 1960*a*; Loopstra & Boldrini, 1966; Loopstra & Rietveld, 1969). Below *ca* 17°C WO_3 is triclinic, space group $P\bar{1}$ (C_i^1) (Braekken, 1931; Tanisaki, 1960*b*), and transforms at about −40°C into another monoclinic phase with space group *Pc* (C_s^2) (Salje, 1976; Tanisaki, 1960*b*). These WO_3 phases have more or less distorted ReO_3-type crystal structures.

Braekken (1931) proposed, as a preliminary result of his structural investigations of CrO_3, MoO_3 and WO_3, a structural model of triclinic tungsten trioxide which has not been refined to date. For a number of reasons it calls for some revision: (1) the crystal structure analysis was performed with twinned crystals of poor quality; (2) only estimated O positional parameters were given; (3) the *c*-axis length of 3·82 (5) Å is half the value as reported in the more recent literature (*e.g.* Tanisaki, 1960*b*) and as found by us; (4) the origin is approximately $0,0,\frac{1}{4}$ from a centre of symmetry; (5) parameters for thermal motion were not considered; (6) it was doubted that triclinic WO_3 has a centrosymmetric crystal structure (Tanisaki, 1960*b*; Schröder, 1976). In the course of a study of the reasons for the electrochromic behaviour of tungsten trioxide (Schirmer, Wittwer, Baur & Brandt, 1977, and references therein) it turned out to be useful to have accurate structural data on triclinic WO_3, which is occasionally encountered at room temperature (Salje & Viswanathan, 1975). Therefore, to gain further insight into the structural chemistry of WO_3 an analysis and refinement of the crystal structure of its triclinic modification was performed by means of single-crystal X-ray diffraction.

Origin of specimen

Starting from a yellowish-white powder (E. Merck), stoichiometric monoclinic WO_3 crystals up to 2 × 2 × 0·5 mm were obtained by sublimation at about 1350°C in an oxidizing atmosphere, following the method of Sawada & Danielson (1959). The greenish-yellow crystals were (001) plates and showed a pronounced domain structure between crossed polarizers with domain walls parallel to (100). Placed in a transparent shallow dish, one monoclinic WO_3 crystal was covered with liquid nitrogen. After evaporation of the liquid it was examined under the microscope during heating-up. At low temperatures the crystal was very light blue with a domain structure oriented about 45° to the room-temperature domain structure. A first spontaneous phase transformation could be observed whereby the colour changed to yellow and the original domain structure reappeared. Subsequently, a second phase transformation without alteration of the domain structure occurred which was recognized by a change in colour to greenish-yellow and a slightly different obliqueness of extinction. Our results of the microscopic inspection of the phase transitions monoclinic → triclinic → monoclinic with increasing temperature are in agreement with Tanisaki's (1960*b*) work. Repeated heating and cooling led to destruction of the WO_3 crystal, which broke into several small pieces due to a distinct change in the unit-cell volume of the different phases. After 20 heating and cooling cycles the crystal was broken into about 40 pieces. Randomly selected specimens were examined by precession photographs and were always found to be triclinic generally yielding two reciprocal lattices due to the two different domain orientations. One crystal piece, however, turned out to be a triclinic single-domain crystal.

Crystal data of triclinic WO_3

Precession photographs of the single-domain WO_3 crystal yielded approximate lattice constants similar to those given by Tanisaki (1960*b*) and also very close to those reported by Loopstra & Rietveld (1969) for the monoclinic room-temperature (RT) modification of WO_3. All angles were found to deviate slightly from 90°. The lattice constants were refined with Guinier powder photographs using Ni-filtered Cu $K\alpha$ radiation (λ = 1·54178 Å) and NaCl (a = 5·6399 Å) as an

Table 1. *Powder data of triclinic* WO_3

Number	$h\,k\,l$	I/I_o	d_o (Å)	d_c (Å)
1	0 0 2	86	3·8375	3·8375
2	0 2 0	98	3·7595	3·7598
3	2 0 0	100	3·6505	3·6536
4	$\bar{1}$ 2 0	9	3·3618	3·3649
5	0 $\bar{2}$ 1	13	3·3458	3·3495
6	$\bar{2}$ 0 1	8	3·3190	3·3192
7	$\bar{1}$ 1 2	7	3·1421	3·1434
8	$\bar{1}$ 2 1	13	3·1153	3·1111
9	1 1 2	18	3·0932	3·0920
10	$\bar{1}$ $\bar{1}$ 2	21	3·0839	3·0832
11	1 $\bar{1}$ 2	8	3·0694	3·0674
12	0 2 2	21	2·7122	2·7135
13	$\bar{2}$ 0 2	36	2·6669	2·6671
14	0 $\bar{2}$ 2	25	2·6592	2·6586
15	$\bar{2}$ 2 0	27	2·6410	2·6412
16	2 0 2	36	2·6268	2·6256
17	2 2 0	24	2·5981	2·5997
18	$\bar{1}$ 2 2	3	2·5616	2·5627
19	$\bar{2}$ 1 2	4	2·5344	2·5343
20	1 2 2	4	2·5261	2·5253
21	$\bar{2}$ 2 1	7	2·5152	2·5174
22	1 $\bar{2}$ 2 $\bar{1}$ $\bar{2}$ 2	7	2·4997	2·4986
23	3 $\bar{1}$ 1 $\bar{3}$ 1 1	3	2·2148	2·2147 2·2142
24	$\bar{2}$ 2 2	17	2·2019	2·2023
25	2 2 2	32	2·1558	2·1555

Table 2. *Crystal data (with monoclinic values in square brackets)*

a	7·309 (2) Å	[7·306 (1) Å]	
b	7·522 (2)	[7·540 (1)]	
c	7·678 (2)	[7·692 (1)]	
α	88·81 (2)°		
β	90·92 (2)	[90·881 (5)°]	
γ	90·93 (2)		
V	421·93 (9) Å^3	[423·68 (7) Å^3]	
Z	8	D_m	7·27 (5) g cm^{-3}
Space group	$P\bar{1}$ (C_i^1)	D_c	7·298
$F(000)$	784	FW	231·8482

internal standard. Powder samples were prepared starting from the monoclinic RT phase which gradually transformed into the triclinic phase by grinding. Extended grinding yielded single-phase powder samples of triclinic WO_3 comprising about 100 sharp lines in the range $0{\cdot}0 \le 2\theta \le 90°$. The powder spectrum listing the first 25 lines is given in Table 1. Line intensities were measured with a Zeiss–Jenoptik photometer and scaled to the value 100 for the strongest reflection. The density was measured with a pycnometer using a triclinic powder sample. All crystal data of triclinic WO_3 are listed in Table 2 (for the space group see below). Lattice constants of the monoclinic RT phase are added for comparison.

Intensity data collection

The single-domain crystal specimen of triclinic WO_3 had dimensions 420 × 60 × 35 μm. For X-ray intensity measurements it was mounted on an automatic four-circle single-crystal diffractometer (CAD-4, Enraf–Nonius). 2452 independent reflections in the range $0{\cdot}0 \le (\sin\theta)/\lambda \le 0{\cdot}93$ Å^{-1} were measured with a NaI (Tl) scintillation counter using Zr-filtered Mo $K\alpha$ radiation (λ = 0·71056 Å) monochromatized by a graphite crystal. After background correction the intensities were further corrected for absorption (μ = 573·6 cm^{-1}), and for Lorentz and polarization factors using the XRAY 70 system of crystallographic programs (Stewart, Kundell & Baldwin, 1970).

Determination and refinement of the structure

Reflection statistics with normalized structure factors (program *NORMSF* of the XRAY 70 system) clearly indicated a centrosymmetric crystal structure for triclinic WO_3. Consequently, the first trial was to determine the crystal structure in space group $P\bar{1}$ (C_i^1) (No. 2 of *International Tables for X-ray Crystallography*, 1965). Because of the very similar lattice constants of triclinic and RT monoclinic WO_3 it appeared reasonable to adapt the positional parameters of the monoclinic structure (Loopstra & Rietveld, 1969) to space group $P\bar{1}$ (C_i^1). Thus, a model of the triclinic crystal structure was obtained with 4 independent W and 12 independent O atoms.

For structure calculations, atomic scattering factors for W^{6+} were taken from Cromer & Waber (1965), those for O^{2-} from Baur (1956). $\Delta f'$ and $\Delta f''$ correction factors for anomalous dispersion (Cromer & Liberman, 1970) were taken into account. Least-squares refinement calculations were performed (program *CRYLSQ* of the XRAY 70 system) starting with rounded positional parameters for all atoms as derived from the results of Loopstra & Rietveld (1969). The function minimized was $\Sigma w||F_o| - |F_c||^2$ with $w = 1/\sigma^2(F_o)$, $\sigma(F_o)$ being the estimated standard deviation (e.s.d.) as obtained from counting statistics. 958 reflections had an F_o less than three times their e.s.d.'s and were treated as 'less-thans' (XRAY 70 system) in the structure refinement. Including individual factors for isotropic thermal motion a reliability index $R = \Sigma||F_o| - |F_c||/\Sigma|F_o|$ of 0·072 was obtained with 'less-thans' omitted and 0·082 with 'less-thans' included. Refinement in the mixed mode using anisotropic temperature coefficients for W and isotropic ones for O, and taking into account an isotropic extinction correction (Larson, 1967), resulted in final R values of 0·050 without 'less-thans' and 0·061 with all reflections (the calculations were terminated when the shift/error value was less than 0·001). Different weighting schemes were applied to the observed structure factors. Best agreement between the sets of F_o and F_c was obtained using unit weights.

Refinement in the noncentrosymmetric space group $P1$ (C_1^1) (No. 1 of *International Tables*, 1965) applying an identical procedure was unsuccessful. The positional and thermal parameters did not converge to a final value. Moreover, four W and six O atoms adopted negative temperature coefficients.

It was concluded that triclinic WO_3 has a centrosymmetric crystal structure. This was supported by investigating the generation of the second harmonic of a pulsed Nd/glass laser (λ 1060 nm, pulse length 300 μs, power density 17 kW cm^{-2}) using a powder sample of triclinic WO_3. At 530 nm no SHG signal could be detected with a photomultiplier which has its maximum sensitivity in this wavelength region of the spectrum. The limit of detection of the apparatus used was about $\frac{1}{5}$ of the SHG signal of quartz powder.

A final ΔF synthesis calculated from the centrosymmetric crystal structure was featureless.*

* A list of structure factors has been deposited with the British Library Lending Division as Supplementary Publication No. SUP 33221 (13 pp.). Copies may be obtained through The Executive Secretary, International Union of Crystallography, 13 White Friars, Chester CH1 1NZ, England.

Table 3. *Positional parameters and thermal coefficients* ($\times 10^4$) *of the triclinic* WO_3 *crystal structure [all atoms in position 2(i)]*

Temperature coefficients are defined as $\exp[-2\pi^2(a^{*2}h^2U_{11} + b^{*2}k^2U_{22} + c^{*2}l^2U_{33} + a^*b^*hkU_{12} + a^*c^*hlU_{13} + b^*c^*klU_{23})]$ for W and $\exp[-2\pi^2U(2\sin\theta/\lambda)^2]$ for O.

	x	y	z	U_{11}	U_{22}	U_{33}	U_{12}	U_{13}	U_{23}
W(1)	2566 (1)	259 (1)	2850 (1)	66 (5)	40 (6)	47 (7)	12 (3)	−8 (3)	−6 (3)
W(2)	2502 (1)	5280 (1)	2158 (1)	60 (5)	40 (6)	55 (7)	10 (3)	−4 (3)	−8 (3)
W(3)	2438 (1)	313 (1)	7817 (1)	60 (5)	49 (6)	52 (7)	11 (3)	0 (3)	0 (3)
W(4)	2499 (1)	5338 (1)	7190 (1)	63 (5)	54 (6)	36 (7)	8 (3)	−6 (3)	−4 (3)

	x	y	z	U (Å^2)		x	y	z	U (Å^2)
O(1)	7 (31)	386 (31)	2100 (32)	142 (42)	O(7)	2186 (29)	2627 (29)	7258 (30)	105 (39)
O(2)	5038 (29)	5361 (29)	2181 (29)	105 (39)	O(8)	2840 (28)	7583 (28)	7679 (28)	83 (36)
O(3)	76 (31)	4660 (31)	2884 (32)	139 (43)	O(9)	2943 (29)	422 (29)	9998 (29)	100 (38)
O(4)	4972 (29)	9638 (29)	2878 (30)	109 (39)	O(10)	2971 (31)	5446 (31)	4982 (32)	139 (43)
O(5)	2851 (28)	2574 (28)	2870 (28)	80 (36)	O(11)	2096 (30)	4820 (30)	9928 (31)	121 (41)
O(6)	2204 (30)	7630 (30)	2232 (30)	113 (40)	O(12)	2088 (28)	9830 (28)	5051 (29)	89 (37)

Table 4. *Bond lengths* (Å) *and angles* (°) *of the independent* WO_6 *octahedra*

$W(1)O_6$ octahedron			$W(2)O_6$ octahedron			$W(3)O_6$ octahedron			$W(4)O_6$ octahedron		
W(1)–O(5)		1·751 (21)	W(2)–O(11)		1·775 (24)	W(3)–O(9)		1·715 (23)	W(4)–O(10)		1·738 (25)
O(12)		1·756 (22)	O(6)		1·787 (22)	O(7)		1·796 (22)	O(8)		1·751 (21)
O(4)		1·826 (21)	O(2)		1·853 (22)	O(1)		1·856 (23)	O(3)		1·881 (25)
O(1)		1·952 (23)	O(3)		1·915 (23)	O(4)		1·974 (21)	O(2)		1·934 (21)
O(6)		2·056 (23)	O(5)		2·116 (21)	O(8)		2·085 (21)	O(7)		2·049 (22)
O(9)		2·215 (23)	O(10)		2·199 (24)	O(12)		2·176 (22)	O(11)		2·157 (24)
O(5)–W(1)–O(9)		87·62 (90)	O(2)–W(2)–O(5)		84·10 (87)	O(7)–W(3)–O(12)		86·24 (92)	O(7)–W(4)–O(10)		94·16 (1·00)
	O(1)	93·34 (96)		O(6)	96·02 (97)		O(9)	101·08 (1·02)		O(11)	78·48 (88)
	O(4)	98·89 (96)		O(10)	81·24 (92)		O(1)	99·89 (1·00)		O(2)	79·50 (88)
	O(12)	100·22 (1·00)		O(11)	99·53 (99)		O(4)	91·83 (94)		O(3)	84·53 (93)
O(9)	O(1)	80·69 (90)	O(5)	O(10)	78·41 (85)	O(8)	O(12)	77·41 (81)	O(8)	O(10)	99·03 (1·04)
	O(4)	83·52 (90)		O(3)	79·57 (89)		O(9)	94·85 (93)		O(11)	88·01 (93)
	O(6)	79·72 (85)		O(11)	93·70 (94)		O(1)	82·73 (92)		O(2)	95·13 (93)
O(1)	O(6)	82·43 (93)	O(6)	O(10)	84·96 (96)		O(4)	81·27 (86)		O(3)	97·49 (98)
	O(12)	95·20 (98)		O(3)	95·66 (99)	O(12)	O(1)	83·40 (93)	O(10)	O(2)	93·06 (1·01)
O(4)	O(6)	82·06 (92)		O(11)	102·85 (1·04)		O(4)	80·46 (85)		O(3)	100·55 (1·06)
	O(12)	98·63 (98)	O(10)	O(3)	81·96 (93)	O(9)	O(1)	100·16 (1·04)		O(7)	81·43 (88)
O(6)	O(12)	92·29 (95)	O(3)	O(11)	95·30 (1·01)		O(4)	94·11 (97)		O(8)	83·18 (93)
O(5)	O(6)	167·13 (96)	O(2)	O(3)	158·57 (99)	O(7)	O(8)	163·08 (94)	O(7)	O(8)	166·03 (95)
O(9)	O(12)	171·39 (88)	O(5)	O(6)	163·17 (95)	O(12)	O(9)	171·09 (91)	O(10)	O(11)	171·47 (98)
O(1)	O(4)	159·57 (1·02)	O(11)	O(10)	170·97 (95)	O(1)	O(4)	159·37 (1·00)	O(2)	O(3)	159·70 (97)

Results

The positional and thermal parameters of the triclinic WO_3 crystal structure are summarized in Table 3. The atomic arrangement represents a pseudocubic ReO_3-type crystal structure and is characterized by corner-sharing distorted O octahedra around the W atoms. The octahedra are tilted towards each other with a tilting component about each of the three coordination axes. A schematic illustration of the corner-sharing octahedra around one unit cell is shown in Fig. 1. The W atoms are appreciably off-centre within the O octahedra and move towards an O triangle. This results in three short and three long W–O bonding distances. As can be seen in Fig. 2, which shows projections of the crystal structure onto the basal planes, short and long

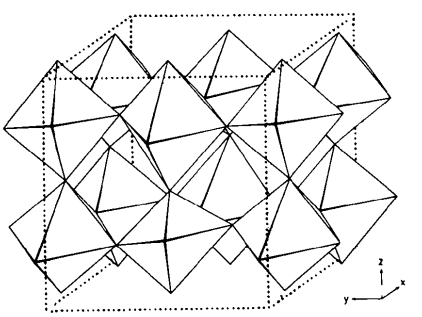

Fig. 1. Corner-sharing O octahedra around one unit cell (outlined by dotted lines) of triclinic WO_3.

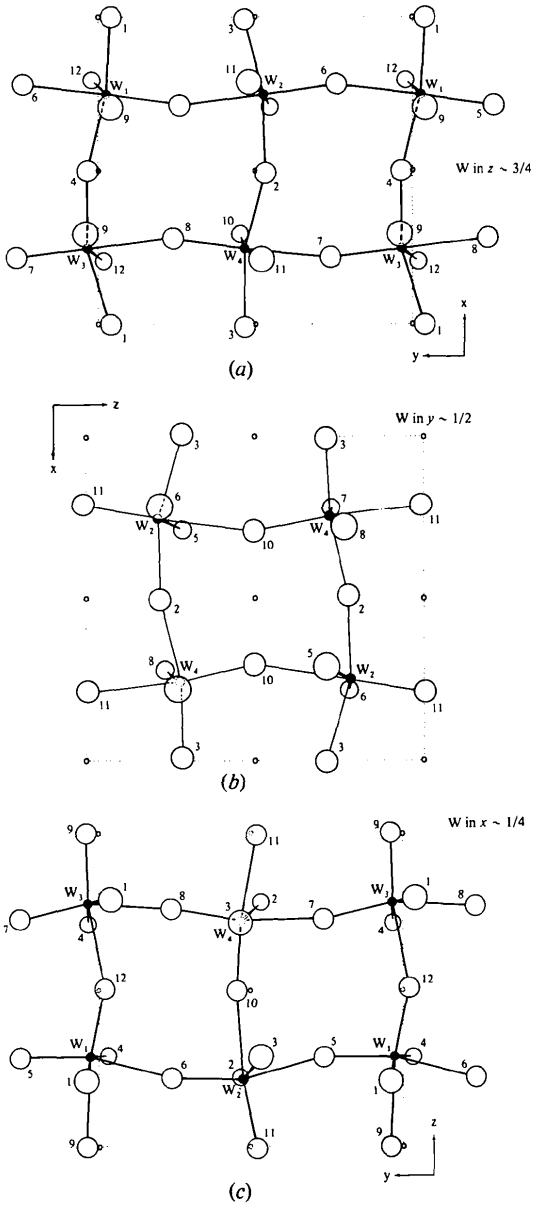

Fig. 2. Projection of the triclinic WO_3 crystal structure onto (*a*) the *ab* plane with W in $z \sim \frac{3}{4}$, (*b*) the *ac* plane with W in $y \sim \frac{1}{2}$, and (*c*) the *bc* plane with W in $x \sim \frac{1}{4}$.

W—O bonds alternate approximately parallel to the coordination axes. Bond lengths and angles of the four symmetrically independent WO_6 octahedra are listed in Table 4. The W—O bonding distance varies from 1·715 to 2·215 Å. It follows from the sum of the ionic radii (W^{6+} 0·64, O^{2-} 1·40 Å) that some of the O ions are considerably polarized by W^{6+}.

Discussion

At first glance and apart from some minor differences, significant deviations of the triclinic from the monoclinic RT crystal structure of WO_3 (Loopstra & Rietveld, 1969) are not observed. However, if the complete sets of atomic positions in the unit cells are listed for comparison, distinct alterations become obvious by means of which the lattice dynamics at the phase-transition point are elucidated. From Table 5 it can be seen how monoclinic and triclinic WO_3 differ from each other. Two O atoms of each of the fourfold Ox(1), Ox(2), Oz(1) and Oz(2) positions of the monoclinic structure (Loopstra & Rietveld, 1969), show drastic deviations from the corresponding triclinic O positions O(2), O(3), O(10) and O(11). The eight pertinent positions are marked in Table 5. The first four O positions differ in *z*, the latter four in *x*. The *y* values are practically unchanged. Since O atoms at only two equipoints of the fourfold monoclinic position show a

Table 5. *Complete set of atomic positional parameters* ($\times 10^4$) *of monoclinic* (*RT*) *and triclinic* WO_3

	Monoclinic (Loopstra & Rietveld, 1969)				Triclinic (this paper)		
	x	*y*	*z*		*x*	*y*	*z*
W(1)	2465	0269	2859	W(1)	2566	0259	2850
	2535	5269	2141	W(2)	2502	5280	2158
	7535	9731	7141	W(1)	7434	9741	7150
	7465	4731	7859	W(2)	7498	4720	7842
W(2)	2538	0353	7807	W(3)	2438	0313	7817
	2462	5353	7193	W(4)	2499	5338	7190
	7462	9647	2193	W(3)	7562	9687	2183
	7538	4647	2807	W(4)	7501	4662	2810
Ox(1)	0025	0350	2106	O(1)	0007	0386	2100
	4975	5350	2894	O(2)	5038	5361	2181
	9975	9650	7894	O(1)	9993	9614	7900
	5025	4650	7106	O(2)	4962	4639	7819
Ox(2)	9974	4636	2161	O(3)	0076	4660	2884
	5026	9636	2839	O(4)	4972	9638	2878
	0026	5364	7839	O(3)	9924	5340	7116
	4974	0364	7161	O(4)	5028	0362	7122
Oy(1)	2840	2605	2848	O(5)	2851	2574	2870
	2160	7605	2152	O(6)	2204	7630	2232
	7160	7395	7152	O(5)	7149	7426	7130
	7840	2395	7848	O(6)	7796	2370	7768
Oy(2)	2099	2568	7318	O(7)	2186	2627	7258
	2901	7568	7682	O(8)	2840	7583	7679
	7901	7432	2682	O(7)	7814	7373	2742
	7099	2432	2318	O(8)	7160	2417	2321
Oz(1)	2827	0383	0046	O(9)	2943	0422	9998
	2173	5383	4954	O(10)	2971	5446	4982
	7173	9617	9954	O(9)	7057	9578	0002
	7899	4617	5046	O(10)	7029	4554	5018
Oz(2)	2856	4840	9944	O(11)	2096	4820	9928
	2144	9840	5056	O(12)	2088	9830	5051
	7144	5160	0056	O(11)	7904	5180	0072
	7856	0160	4944	O(12)	7912	0170	4949

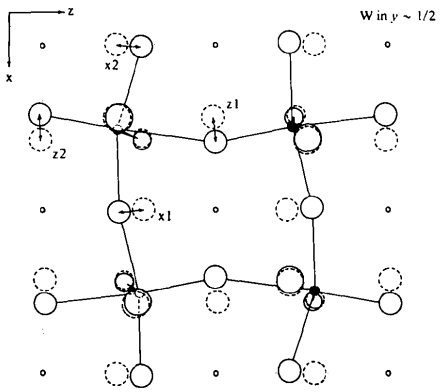

Fig. 3. Simultaneous projection of the crystal structures of triclinic and monoclinic WO_3 onto the *ac* plane with W in $y \sim \frac{1}{2}$ [full circles: O positions in the triclinic structure (see Fig. 2*b*); broken circles: O positions in the monoclinic structure].

pronounced shift in the x or z directions, it is concluded that the results of Loopstra & Rietveld (1969) cannot be in error. Fig. 3 shows a projection of both the triclinic and monoclinic crystal structures on the same *ac* plane around W at $y \sim \frac{1}{2}$. Full circles indicate the O positions of the triclinic, broken circles of the monoclinic structure.

The transformations at the monoclinic–triclinic phase transition mainly occur at the O positions $x(1)$, $x(2)$, $z(1)$ and $z(2)$. The movement is characterized by a tilt of the O octahedra with tilt axes parallel to y. The tilt angle is near 17°, which corresponds to a maximum linear atomic shift of about 0·54 Å for the indicated O positions. Compared with the hypothetical high-symmetry phase $\{x[Oz(2)] = x[Oz(1)] = z[Ox(2)] = z[Ox(1)] = \frac{1}{4}\}$ the tilts of the monoclinic phase just change sign: the octahedron around W(2) is tilted in the monoclinic phase by *ca* 9° counter-clockwise and in the triclinic phase by nearly the same angle in the opposite direction. The same O–W–O chains in the xz plane can be obtained for both phases by a shift of the origin in the direction z by $\frac{1}{4}$. This shift transforms the O–W–O chains near to the tilt axes parallel to y incongruently. Therefore, the phase transition is described by a spontaneous tilt of the O octahedra, giving rise to a phase shift of the deformation vectors in the xz plane against those near the tilt axes. This spontaneous tilt is generally accompanied by a temperature hysteresis which occasionally allows the existence of the triclinic WO_3 structure at room temperature.

The tilt angle of the O octahedra is the critical parameter during the phase transformation, the interatomic distances and angles remaining almost unchanged. This is supported by the very small changes of phonon frequencies at the phase-transition point (Salje, 1975). With the structural tilt angle as an order parameter a continuous slowing down of the correlated phonon branches is expected. As the dimensions of the unit cell are practically unchanged during the transformation, these critical phonons are zone centre modes and observable in the Raman experiment. Experimentally, no continuous shift was found, unlike the monoclinic–orthorhombic transformation at higher temperatures. Furthermore, the decrease of the frequencies of the 30 and 60 cm^{-1} modes and the disappearance of the 610 cm^{-1} band occur spontaneously, indicating first-order transformation behaviour. Whereas the frequency shift can be interpreted as being due to the spontaneous shift of the tilt angle resulting in a spontaneous change of phonon–phonon interaction, this seems to be unlikely in the case of the 610 cm^{-1} band. In the spectrum this band is near to the 719 and 808 cm^{-1} Slater modes, which are closely related to the direct W–O force constants. Hence these modes depend very sensitively on variations of the W–O distances and interaction energies. During the phase transition both modes are almost unchanged, in accordance with the present structure analysis. Thus, the disappearance of the 610 cm^{-1} band must be correlated either by changes of mode parities or by second-order phonon–phonon interactions. The change of parity demands the noncentrosymmetric space group $P1$ and is therefore in contrast to the space group $P\bar{1}$. It is planned to examine the second-order character of the 610 cm^{-1} band by measuring the pressure dependence of Raman lines in the triclinic phase.

We are indebted to W. Littke (Chemistry Institute, University of Freiburg) for his assistance and permission to use the CAD-4 diffractometer. The careful technical assistance of F. Friedrich is gratefully acknowledged. All computations were performed on the Univac 1108 computer of the Rechenzentrum of Freiburg University. This paper is based on work supported by the Bundesministerium für Forschung und Technologie under Contract NT. 647.

References

BAUR, W. H. (1956). *Acta Cryst.* **9**, 515–519.
BRAEKKEN, H. (1931). *Z. Kristallogr.* **78**, 484–488.
CROMER, D. T. & LIBERMAN, D. (1970). *J. Chem. Phys.* **53**, 1891–1898.
CROMER, D. T. & WABER, J. T. (1965). *Acta Cryst.* **18**, 104–109.
International Tables for X-ray Crystallography (1965). Vol. I, 2nd ed. Birmingham: Kynoch Press.
KEHL, K. L., HAY, R. G. & WAHL, D. (1952). *J. Appl. Phys.* **23**, 212–215.
LARSON, A. C. (1967). *Acta Cryst.* **26**, 664–666.
LEVKOWITZ, I., DOWELL, M. B. & SHIELDS, M. A. (1975). *J. Solid State Chem.* **15**, 24–39.
LOOPSTRA, B. O. & BOLDRINI, P. (1966). *Acta Cryst.* **21**, 158–162.
LOOPSTRA, B. O. & RIETVELD, H. M. (1969). *Acta Cryst.* B**25**, 1420–1421.

RAO, C. N. R. & RAO, G. V. S. (1974). *Natl Stand. Ref. Data Ser. Natl Bur. Stand.* **49**, 117–122.
SALJE, E. (1975). *Acta Cryst.* A**31**, 360–363.
SALJE, E. (1976). *Ferroelectrics*, **12**, 215–217.
SALJE, E. (1977). *Acta Cryst.* B**33**, 574–577.
SALJE, E. & VISWANATHAN, K. (1975). *Acta Cryst.* A**31**, 356–359.
SAWADA, S. & DANIELSON, G. C. (1959). *Phys. Rev.* **113**, 803–808.
SCHIRMER, O. F., WITTWER, V., BAUR, W. & BRANDT, G. (1977). *J. Electrochem. Soc.* **124**, 749–753.
SCHRÖDER, F. A. (1976). *Acta Cryst.* A**32**, 342–344.
STEWART, J. M., KUNDELL, F. A. & BALDWIN, J. C. (1970). The XRAY 70 system. Computer Science Center, Univ. of Maryland, College Park, Maryland.
TANISAKI, S. (1960*a*). *J. Phys. Soc. Jpn*, **15**, 573–581.
TANISAKI, S. (1960*b*). *J. Phys. Soc. Jpn*, **15**, 566–573.

Acta Cryst. (1978). B**34**, 1111–1116

Antimony Trichloride 1:1 Complexes with Terephthaldehyde and *p*-Diacetylbenzene

BY WILLIAM A. BAKER AND DONALD E. WILLIAMS

Department of Chemistry, University of Louisville, Louisville, Kentucky 40208, *USA*

(*Received* 29 *March* 1977; *accepted* 20 *July* 1977)

The crystal and molecular structures of 1:1 adducts of $SbCl_3$ with organic carbonyl compounds were determined by X-ray diffraction. The terephthaldehyde adduct ($C_8H_6O_2SbCl_3$) crystallized in space group *Pnma* with $Z = 4$ and lattice constants $a = 8{\cdot}433$ (1), $b = 21{\cdot}556$ (2), and $c = 6{\cdot}279$ (1) Å. The Sb atom is strongly coordinated to two carbonyl O atoms, and weakly coordinated to a Cl, in a distorted pentagonal bipyramidal configuration. The *p*-diacetylbenzene adduct ($C_{10}H_{10}O_2SbCl_3$) crystallized in space group *Pbca* with $Z = 8$ and lattice constants $a = 17{\cdot}689$ (2), $b = 17{\cdot}639$ (2), and $c = 8{\cdot}996$ (2) Å. In this structure there are two kinds of *p*-diacetylbenzene molecules, of which one has coplanar acetyl groups and one has acetyl groups non-coplanar by 9·9°. The Sb atom is strongly coordinated to two carbonyl O atoms and to a Cl in a distorted octahedral configuration.

Introduction

Over a half century ago Menshutkin (1912) reported the existence of over 60 compounds which were adducts of antimony trichloride with organic molecules. Recently, Park (1969) has examined 119 adducts formed between antimony trichloride and various organic molecules. The detailed crystal structures of several adducts have been determined. These include 2:1 adducts with naphthalene (Hulme & Szymanski, 1969) and phenanthrene (Demaldé, Mangia, Nardelli, Pelizzi & Tani, 1972) and a 1:1 adduct with aniline (Hulme & Scruton, 1968).

Antimony trichloride itself has a pyramidal structure both in the crystal (Lindquist & Niggli, 1956) and in the gas phase observed by electron diffraction (Allen & Sutton, 1950) or microwave spectroscopy (Kisliuk, 1954). Although antimony trichloride is in Group V of the periodic table and has a lone pair of electrons on Sb, its normal mode of coordination is in the role of electron acceptor from the coordinated ligand atoms.

Experimental

The 1:1 $SbCl_3$–terephthaldehyde adduct ($C_8H_6O_2$-$SbCl_3$) was prepared (Park, 1969) by addition of 2·0 g of terephthaldehyde (Aldrich Chemical Co., m.p. 114–115 °C) to a dry solution of 3·7 g $SbCl_3$ (Baker Chemical Co., further purified by vacuum sublimation) in 100 ml CCl_4. The mixture was boiled and filtered. The resulting white crystals were recrystallized from CCl_4, m.p. 79–81 °C. The density measured by flotation in CBr_4–CCl_4 solution was 2·05 g cm^{-3}; the calculated density was 2·11 g cm^{-3}. X-ray intensity data were taken from a single crystal of approximate dimensions 0·3 × 0·3 × 0·4 mm sealed in a glass capillary tube. Lattice constants were obtained by a least-squares fit (Williams, 1964) using the Nelson & Riley (1945) extrapolation function to ten high-angle reflections observed with Cr $K\alpha$ ($\lambda = 2{\cdot}28962$ Å) radiation.

The diffraction symmetry was orthorhombic and the systematically absent reflections indicated space groups